Photonic approach to microwave frequency measurement with extended range based on phase modulation

Xiuyou Han (韩秀友)*, Siteng Zhang (张思藤), Chao Tong (佟 超), Nuannuan Shi (石暖暖), Yiying Gu (谷一英), and Mingshan Zhao (赵明山)

Photonics Research Center, School of Physics and Optoelectronic Engineering, Dalian University of Technology, Dalian 116024, China

**Corresponding author: xyhan@dlut.edu.cn*

Received December 12, 2012; accepted January 25, 2013; posted online April 24, 2013

We propose and demonstrate a photonic approach to instantaneous frequency measurement with an extended range based on phase modulation. In the measurement system, two optical wavelengths and two dispersion fiber segments are used to construct the frequency-dependent amplitude comparison functions (ACFs). Several ACFs can be utilized jointly to determine the microwave frequency without ambiguities beyond a monotonic region of the lone conventional ACF. The measurable range of microwave frequency can be extended and the accuracy can be improved by selecting an ACF with a large slope. The experimental results show that the errors are limited within ±140 MHz of a frequency measurement range from 8 to 20 GHz.

OCIS codes: 060.0060, 060.5060, 060.5625.
doi: 10.3788/COL201311.050604.

The frequency measurement of input microwave signals is very important for modern radar warning receivers in the field of electronic warfare (EW)[1]. Unlike conventional receivers, the input signals of EW receivers are unknown. Estimate the frequency of the unknown signal in a very short period of time is desirable, a method known as instantaneous frequency measurement (IFM). Considering the frequencies of modern radar systems range from subgigahertz to millimeter waves, the conventional electrical implementations may not meet the requirements for a wide operating frequency range and a nearly real-time response.

Photonic techniques can overcome these limitations, given such advantages as a wide instantaneous bandwidth, light weight, low loss, and immunity to electromagnetic interference[2,3]. A number of approaches have been proposed in the past few years to measure the microwave frequency in the optical domain[4−14]. Optical power or microwave power monitoring is usually performed to determine the unknown frequency. With optical power, a sinusoidal filter[4,5], channelization filter[6], phase shift filter[7] or scanning filter[8,9] is used to map the frequency information into the change of optical power, which may reduce the system cost, thereby fulfilling the requirement of a low-speed photodetector (PD). With microwave power, on the other hand, dispersion-induced microwave power variations are mostly adopted to establish a frequency-dependent amplitude comparison function (ACF)[10−14], which can derive the frequency with a wide measurable range and high accuracy.

Intensity modulation using Mach-Zehnder modulators (MZMs) is usually applied in the photonic IFM links[10,11]. The major difficulty associated with MZMs is the need for a sophisticated DC bias-controlled electrical circuit to stabilize the operation of the MZMs[15]. The phase modulators (PMs) can appropriately eliminate the bias drifting problem. Recently, PMs have attracted more and more attentions in microwave-photonic systems besides the IFM links[12−14]. For the ACF-based IFM technique with phase modulation, the measurable frequency range is generally limited to a monotonic region of ACF to avoid ambiguities[12].

In this letter, a photonic approach to microwave frequency measurement with an extended range based on phase modulation is proposed. In the measurement system, multiple photonic links with phase modulation are established. Using the microwave signal power fading effect induced by the dispersive medium, several ACFs can be used jointly to determine the microwave frequency without ambiguities beyond a monotonic region with only one ACF. The measurable range of the microwave frequency can be extended, and the accuracy can be improved with the proper selection of ACF with a large slope. The operation principle of the photonic approach for IFM is illustrated, and a proof-of-concept experiment is performed to verify the feasibility of the approach.

The schematic diagram of the proposed photonic IFM approach is shown in Fig. 1. The lightwaves with different wavelengths from two laser diodes (LDs) are combined in a multiplexer and sent to the PM. The unknown input microwave signal is modulated on the two lightwaves simultaneously. After transmitting through the first dispersive fiber l_1, the two lightwave signals are split equally into two paths by a 3-dB coupler. The two lightwave signals in the upper path are demultiplexed directly and detected by the PDs, respectively. The lower

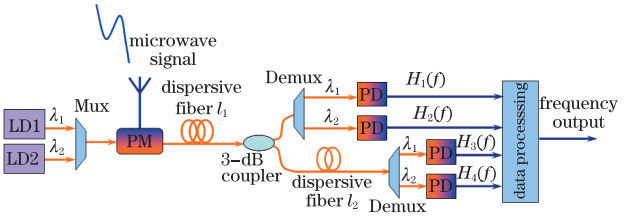

Fig. 1. Schematic diagram of the proposed photonic approach for microwave frequency measurement.

 © 2013 Chinese Optics Letters

path is connected with the second dispersive fiber l_2, and the two lightwave signals in the lower path are demultiplexed and detected by the PDs, respectively. The output microwave signal power values from the four PDs are digitized and compared in a data processing unit. Given the chromatic dispersion of fiber links the phase modulation to intensity modulation, conversion occurs[16], and the frequency-dependent ACFs can be constructed. Unlike previous methods, the proposed IFM system determines the microwave frequency by simultaneously utilizing several ACFs via a simple search algorithm. Each ACF becomes multivalued because of the periodic behavior of dispersion induced power fading with a few ambiguous frequency solutions. The algorithm searches all the solutions of each ACF and selects the intersection of potential frequency solutions of different ACFs, which is unique by optimal design the wavelengths and the dispersive fiber lengths. Thus, the measurable frequency range can be extended without restricting it to the frequencies where the ACF is monotonic.

The output microwave signal power from PDs, as shown in Fig. 1, can be expressed as[16]

$$H_n = \eta_n \sin^2\left(\frac{\pi f^2 \lambda_n^2 D_n L_n}{c}\right), \quad n = 1, 2, 3, 4, \tag{1}$$

where c is the light speed in vacuum; f is the input microwave frequency; λ_n is the wavelength of the lightwave; D_n is the chromatic dispersion coefficient corresponding to the optical wavelength λ_n; L_n is the dispersive fiber length ($L_{1,2} = l_1$ and $L_{3,4} = l_1 + l_2$ for the upper and lower paths, respectively); η_n is the response parameter of the photonic link, which is a function of the output optical power of LD, input microwave signal power, responsivity of PD, insertion loss of PM, fiber, multiplexer, demultiplexer, and 3-dB coupler.

Based on the detected microwave signal power of the four photonic links, the different ACFs in dB can be expressed as

$$\mathrm{ACF}_{ij} = 10\log\left(\frac{H_i}{H_j}\right) = 10\log\left[\frac{\sin^2(\frac{\pi f^2 \lambda_i^2 D_i L_i}{c})}{\sin^2(\frac{\pi f^2 \lambda_j^2 D_j L_j}{c})}\right] + \gamma_{ij}, \tag{2}$$

where γ_{ij}=10log(η_i/η_j) is the ratio of the response parameters of different photonic links, which is independent of the power and frequency of the input microwave signal. When the output optical powers of the two LDs are the same, and the responsivities of the four PDs are uniform, there are $\gamma_{12} = \gamma_{34}$=0 and $\gamma_{13} = \gamma_{23} = \gamma_{14} = \gamma_{24} = \gamma_{\mathrm{C}}$. γ_{C} is the extra loss of the lower path (links 3 and 4) compared with upper path (links 1 and 2), which is caused by the inherent loss of dispersive fiber l_2 ($\alpha_{\mathrm{F}} \cdot l_2$, α_{F} is the loss factor of the dispersive fiber) and the splice loss between dispersive fiber l_2 and 3-dB coupler (α_{S}). However, γ_{ij} is constant for the established measurement system; thus, it has no influence on the frequency determination for the ACFs.

The main parameters of the proposed measurement system, wavelengths and fiber lengths, should be designed carefully to achieve the desired results. The wavelength space of the two LDs should be large enough to utilize the dispersion-dependent property of ACFs. The lengths of the two fiber segments should also be chosen properly. Based on Eq. (1), for the single-mode-fibers (SMFs) with fixed chromatic dispersion coefficients, the longer length will induce a sharp curve for the output microwave power versus frequency; thus, the lower frequency can be estimated accurately by the first monotonic region of the ACF curve. In addition, the monotonic regions of the multiple ACFs curves should be interleaved evenly to extend the measurable frequency range.

The calibration ACFs in the look-up table can be measured or calculated from the total chromatic dispersion in the wavelengths of the two LDs. As an example of the frequency estimation process using the calibration ACFs, Fig. 2 shows the calculated ACF_{12} and ACF_{23} with λ_1=1 525 nm and λ_2=1 605 nm, two MF segments (α_F=0.2 dB/km) with l_1=25 km and l_2=32 km, $D_1 = D_3$=15.06 ps/(nm·km) @ 1 525 nm, $D_2 = D_4$=19.57 ps/(nm·km) @1 605 nm (the dispersion values of SMFs are measured using phase shift method[17,18]), and the splice loss α_S=0.1 dB between dispersive fiber l_2 and 3-dB coupler. When an unknown microwave signal (13.11 GHz) is inputted to the measurement setup, the values of ACF_{12} (2.32 dB) and ACF_{23} (17.84 dB) can be obtained through the detected powers. The possible frequency is 13.11 or 16.54 GHz based on the look-up table of ACF_{12}. Based on the look-up table of ACF_{23}, the possible frequency is 11.00, 13.11, 18.86, or 18.06 GHz. The actual frequency can be determined by determining the intersection of the two sets of possible frequencies. The look-up table of ACF_{23} is then used to estimate the frequency of the unknown input microwave signal because the slope of the ACF_{23} curve at around 13 GHz is larger than that of ACF_{12} curve in the monotonic range, and the measurement accuracy is higher. Moreover, another ACF_{ij} can also be used if its slope is larger than that of ACF_{23} curve.

A proof-of-concept experiment is implemented based on the configuration as shown in Fig. 1. Two lightwaves from two CW lasers (λ_1=1 525 nm and λ_2=1 605 nm, respectively, each with 5 dBm of optical power) are phase modulated via the PM (EO-Space, bandwidth of 20 GHz) using a microwave signal with an unknown frequency. For simplicity, a microwave signal of 0 dBm with a frequency tunable from 2 to 20 GHz is generated by a signal generator (Agilent 8267D). The two SMF segments are l_1=25 km and l_2=32 km in series. The demultiplexed phase modulated signals are detected by PDs (u^2t 2120R) at the output of the four photonic links. The Labview program is used to record data from the scanned microwave

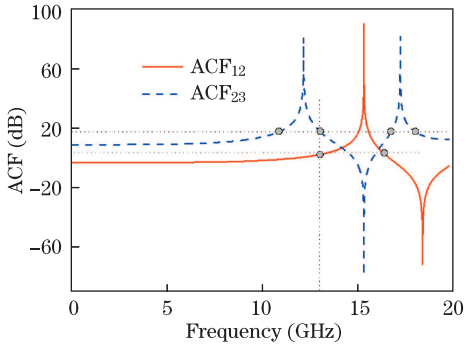

Fig. 2. Frequency estimation with ACFs (ACF_{12}, ACF_{23}) from the power variation response of photonic links 1, 2, and 3.

frequency and the detected microwave signal power. The radio frequency is subsequently estimated.

In the experiment, the power distribution functions of the four photonic links are first measured, with which the calibration ACFs are constructed. Here, three ACFs, namely ACF_{12}, ACF_{23}, and ACF_{34} versus frequency, as shown in Fig. 3, are selected and stored in the look-up table. The theoretical ACFs are also plotted in Fig. 3, which demonstrates the measured results are consistent with the theoretical ones. We further tune the frequency of the input microwave signal and estimate its frequency with the search algorithm presented before. As an example of data processing, the ACF values of an input microwave signal of 11.0 GHz are marked with dotted lines in each ACF curve, as shown in Fig. 3. Although multiple possible frequencies can be produced by each ACF, the potential frequency can be confirmed at approximately 11.0 GHz after the intersection processing of the possible frequencies. ACF_{34} is used to estimate the input microwave frequency as 11.01 GHz because the slope of its curve around the potential frequency is the largest of the slopes of the three ACF curves.

The system has been tested for microwave signals between 8 and 20 GHz. As shown in Fig. 4, the system is able to determine unambiguously the frequency of the microwave signal. The measurement errors calculated by comparing the measured and input frequencies are shown

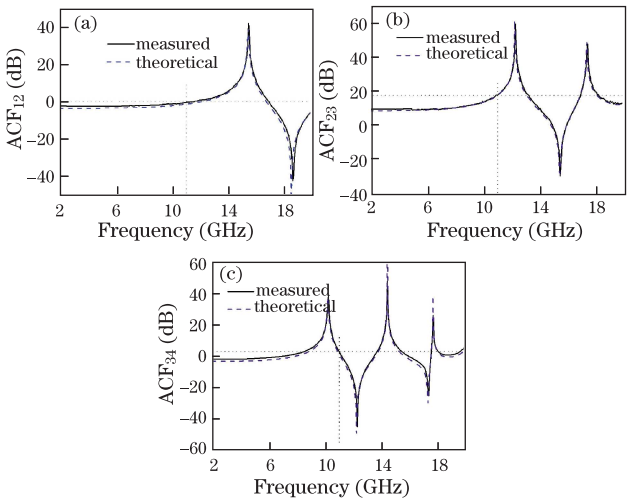

Fig. 3. ACF functions of (a) ACF_{12}, (b) ACF_{23}, and (c) ACF_{34} with l_1 =25 km, l_2 =32 km, λ_1 =1 525 nm, and λ_2 =1 605 nm. Dotted lines illustrate the frequency estimation of an 11.0-GHz input microwave signal.

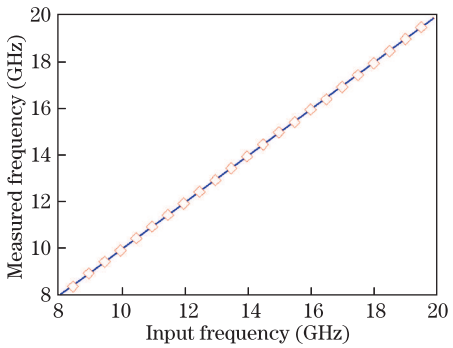

Fig. 4. Measured frequency versus input frequency.

in Fig. 5. The measurement errors are within ±140 MHz for the frequency range of 8–20 GHz (the maximum absolute error is 140 MHz at 8 GHz, i.e. 1.75%). The measurement accuracy is improved since the system can operate in an ACF region with a large slope and is therefore comparable to previously reported systems[9−11], which is acceptable for applications where a rough but instantaneous microwave frequency estimation is required.

The upper frequency bound in the experiment is limited by the devices and equipment available in the lab. The lower frequency bound is given by the small slope of the ACFs at lower frequencies, where changes of the ACF are minimal. The lower limit can be reduced by changing the total dispersion of the setup to reduce the frequency of the first maximum of the recovered power with dispersion fading. The best accuracy range is obtained in the frequency range corresponding to the larger slopes in the ACFs.

To obtain a near real-time system, the data processing unit has to compensate for the different time delays between photonic links 1-2 and 3-4. In the experiment, the time delay between the upper and lower photonic links is about 0.15 ms for the second SMF segment of 32 km. This time delay, together with the time delay needed for processing, will add a time lag to the system.

Some sources of measurement errors, such as the fluctuation of the total dispersion of the SMFs due to the environmental temperature changes and the wavelength stability of the LDs, have been identified.

Temperature changes result in a slight change in the chromatic dispersion coefficient of the fiber, thereby degrading system performance. For the typical operation temperature from –40 to +85 °C, the effect of temperature variation on the frequency measurement (input microwave frequency of f=14.0 GHz) of the case of SMF is shown in Fig. 6, where the chromatic dispersion at room temperature (25 °C) is assumed as the reference, and a typical dispersion variation with a temperature of –0.003 ps/(nm·km·°C)[19] is considered. The temperature increase induces a smaller measured frequency because of the negative temperature-dependent dispersion of the SMF. For a cost effective measurement system, the uncooled distributed feedback grating laser diodes (DFB-LDs) may be used as light sources. The wavelength drift of uncooled DFB-LD is about 0.08 nm/°C[20]. The wavelength drift is about –5.2–4.8 nm for above typical operation temperature. Figure 7 shows the effect of the wavelength drift of the light source on the frequency measurement. The slope of the frequency error curve induced by the temperature-dependent wavelength is opposite to that of the frequency error curve induced by the temperature-dependent chromatic dispersion. Consequently, the combined effect on the measurement frequency error can be decreased to some extent, as shown in Fig. 8.

In the actual application, the power of the microwave received by the antenna may vary and may usually be small. Here, the frequencies with the microwave powers of 0, –4, –8, and –12 dBm are measured by the experimental system. The results are shown in Fig. 9. A lower microwave power results in a larger measurement error, possibly because of the small output microwave power (–50 dBm output power; –12 dBm input power) from

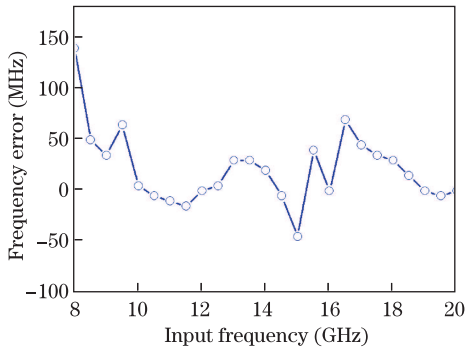

Fig. 5. Measurement error as a function of input frequency.

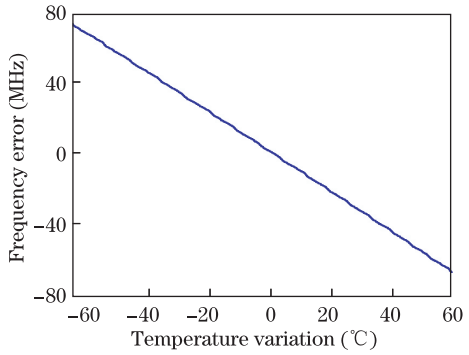

Fig. 6. Frequency error caused by the dependence on the chromatic dispersion temperature.

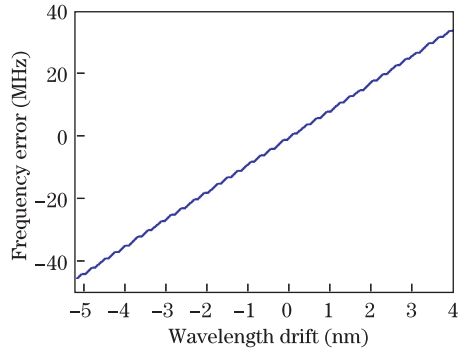

Fig. 7. Frequency error caused by the wavelength drift of the light source.

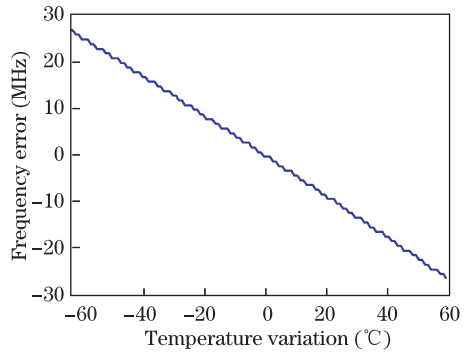

Fig. 8. Frequency error caused by both the temperature-dependent chromatic dispersion of the SMF and wavelength of the light source.

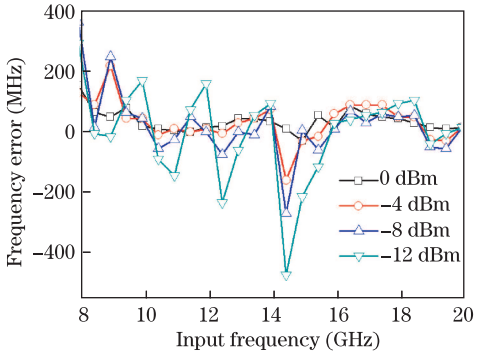

Fig. 9. Frequency error with different input microwave powers.

the photonic links which have sustained a large optical loss and extra noise. An electronic amplifier at the input of the PM or an optical amplifier in the photonic links can be used to improve the measurement accuracy.

In conclusion, a novel approach to improve the frequency range and accuracy of photonic-based IFM systems is proposed. The measurement theory and search algorithm are analyzed. The combination of ACFs yields a measurement error of ±140 MHz over a frequency range of 8–20 GHz, which are obtained experimentally and overcomes the limitation of the measurable frequencies to a monotonic region with only one ACF. The measurement frequency error caused by temperature-dependent chromatic dispersion of the SMF and wavelength of the light source is analyzed. The result shows that the combined effect can decrease the error to some extent. The frequency measurement with different input microwave powers is tested. The potential factors inducing measurement errors are analyzed and solutions are suggested. The photonic approach to microwave frequency measurement may meet the demand of future EW receivers.

This work was supported by the National Natural Science Foundation of China (No. 60807015), the National "863" Program of China (No. 2012AA040406), the Natural Science Foundation of Liaoning Province (No. 20102020), and the Fundamental Research Funds for the Central Universities.

References

1. D. C. Schleher, *Electronic warfare in the information age* (Artech House Publishers, London, 1999).
2. J. Capmany and D. Novak, Nat. Photon. **1,** 319 (2007).
3. J. P. Yao, J. Lightwave Technol. **27,** 314 (2009).
4. H. Chi, X. H. Zou, and J. P. Yao, IEEE Photon. Technol. Lett. **20,** 1249 (2008).
5. J. Dong, Y. Yu, X. Zhang, and D. Huang, Chin. Opt. Lett. **9,** 051202 (2011).
6. S. T. Winnall, A. C. Lindsay, M. W. Austin, J. Canning, and A. Mitchell, IEEE Trans. Microwave Theory Technol. **54,** 868 (2006)
7. X. H. Zou, W. Pan, B. Luo, L. S. Yan, and Y. S. Jiang, Opt. Express **19,** 24712 (2011).
8. H. L. Guo, G. Z. Xiao, N. Mrad, and J. P. Yao, IEEE Photon. Technol. Lett. **20,** 45 (2009).
9. P. Rugeland, Z. Yu, C. Sterner, O. Tarasenko, G. Tengstrand, and W. Margulis, Opt. Lett. **34,** 3794

(2009).

10. L. V. T. Nguyen and D. B. Hunter, IEEE Photon. Technol. Lett. **18,** 1188 (2006).
11. X. H. Zou and J. P. Yao, IEEE Photon. Technol. Lett. **20,** 1989 (2008).
12. X. M. Zhang, H. Chi, X. M. Zhang, S. L. Zheng, X. F. Jin, and J. P. Yao, IEEE Microwave Wireless Component Lett. **19,** 422 (2009).
13. J. Q. Zhou, S. N. Fu, P. P. Shum, S. Aditya, L. Xia, J. Q. Li, X. Q. Sun, and K. Xu, Opt. Express **17,** 7217 (2009).
14. J. Q. Zhou, S. N. Fu, S. Aditya, P. P. Shum, and C. Lin, IEEE Photon. Technol. Lett. **21,** 1069 (2009).
15. S. Gronbach, "Method and apparatus for controlling a bias voltage of a Mach–Zehnder modulator", U. S. patent 7075695 (2006).
16. H. Chi and J. P. Yao, IEEE Photon. Technol. Lett. **20,** 315 (2008).
17. B. Costa, D. Mazzoni, M. Puleo, and E. Vezzoni, IEEE J. Quantum Electron. **QE-18,** 1497 (1982).
18. EIA/TIA-455-169A (FOTP-169), "Chromatic dispersion measurement of single mode optical fiber by the phase shift method".
19. J. H. Michael, W. John, H. Michael, and B. Bob, IEEE Photon. Technol. Lett. **14,** 1524 (2002).
20. H. Zhao, H. Chi, Q. Zeng, S. Xiao, and M. Jiang, Proc. SPIE **4908,** 183 (2002).